



Vital role of oxidative stress in tadpole liver damage caused by polystyrene nanoparticles

Hao Zang^a, Cenxi Zhao^a, Runqiu Cai^a, Haiyan Wu^a, Liutao Wei^a, Chaoyu Zhou^a, Jie Chai^b, Xuepeng Teng^{b,*}, Tianlong Liu^{a,*}

^a National Key Laboratory of Veterinary Public Health and Safety, College of Veterinary Medicine, China Agricultural University, Beijing 100093, China

^b Shandong Cancer Hospital and Institute, Shandong First Medical University and Shandong Academy of Medical Sciences, Jinan 250117, China



ARTICLE INFO

Handling Editor: Dr Hyo-Bang Moon

Keywords:

Polystyrene nanoparticles
Tadpoles
Bioaccumulation
Liver damage
Oxidative stress

ABSTRACT

Polystyrene nanoparticles are emerging as contaminants in freshwater environments, posing potential risks to amphibians exposed to extended periods of water contamination. Using tadpoles as a model, this study aimed to evaluate the toxicity of PS NPs. Pyrolysis-gas chromatography-tandem mass spectrometry (Py-GCMS) analysis revealed a concentration-dependent increase in polystyrene nanoparticles (PS NPs) levels in tadpoles with escalating exposure concentrations. Following exposure to 100 nm fluorescent microspheres, fluorescence was observed in the intestines and gills, peaking at 48 hours. Histopathological analysis identified degenerative necrosis and inflammation in the liver, along with atrophic necrosis of glomeruli and tubules in the kidneys. These results indicate a discernible impact of PS NPs on antioxidant levels, including reduced superoxide dismutase and catalase activities, elevated glutathione content, and increased malondialdehyde levels. Electron microscopy observations revealed the infiltration of PS NPs into Kupffer's cells and hepatocytes, leading to visible lesions such as nuclear condensation and mitochondrial disruption. The primary objective of this research was to elucidate the adverse effects of prolonged PS NPs exposure on amphibians.

1. Introduction

Plastics persist in even the most remote marine and polar regions. (North and Halden, 2013) Given its widespread production and use, plastic is recognized as an emerging pollutant, raising significant concerns about its potential adverse effects. (Aragaw, 2020; Khalid et al., 2021) Polystyrene (PS) poses a threat to human well-being, as the human body is exposed to microplastics through inhalation of air and dust, as well as dermal contact with various everyday items. (Prata et al., 2020) Furthermore, PS has been shown to upregulate crucial factors affecting gastric disorders in humans, including the expression of IL-6 and IL-8 genes. (Forte et al., 2016)

The slow breakdown of microplastics can lead to long-term environmental damage, with particularly severe pollution in oceans and rivers. (O'Brine and Thompson, 2010, Peng et al., 2017; Gray et al., 2018) Research has demonstrated that aquatic creatures, including zooplankton (Cui et al., 2017), invertebrates, amphibians, and fish, are

adversely affected by the ingestion, inhalation, and penetration of microplastics. (Harding, 2016; Lusher et al., 2017; Verla et al., 2019) The digestive system is particularly vulnerable to the impact of PS, with adult zebrafish exhibiting increased inflammatory factors in the gastrointestinal tract, leading to microbiota dysbiosis and inflammation. (Jin et al., 2018) Additionally, PS induces hepatitis, and oxidative stress in the liver (Yu et al., 2018), and has the potential to disturb lipid and energy metabolism. (Lu et al., 2016b)

Previous experiments have also shown that PS can impact the reproduction of freshwater organisms. (Murphy and Quinn, 2018) In oysters, the presence of microplastics leads to a reduction in the number and size of oocytes and a significant decrease in sperm velocity, profoundly affecting offspring development. (Sussarellu et al., 2016) Sea urchins, zebrafish, and *Daphnia magna* embryos exhibit a substantial transgenerational influence of PS. (Della Torre et al., 2014; Pacheco et al., 2018)

Currently, specific nanomaterials play a pivotal role as innovative

Abbreviations: PS NPs, Polystyrene; Py-GCMS, Pyrolysis-gas chromatography-tandem mass spectrometry; PS NPs, Polystyrene nanoparticles; SOD, superoxide dismutase; CAT, Catalase CAT; MDA, Malondialdehyde; GSH, glutathione.

* Corresponding authors.

E-mail addresses: tengxuepeng@163.com (X. Teng), liutianlong@mail.cau.edu.cn (T. Liu).

<https://doi.org/10.1016/j.ecoenv.2024.116331>

Received 16 December 2023; Received in revised form 25 March 2024; Accepted 12 April 2024

Available online 19 April 2024

0147-6513/© 2024 The Authors. Published by Elsevier Inc. This is an open access article under the CC BY license (<http://creativecommons.org/licenses/by/4.0/>).

and environmentally friendly catalysts for organic materials, while also serving as useful indicators of pollutant presence. (Zinatloo-Ajabshir and Salavati-Niasari, 2019; Khayoon et al., 2023, Zinatloo-Ajabshir et al., 2024a; 2024b) Simultaneously, the utilization of eco-friendly and renewable nanomaterials holds great potential to significantly reduce the associated environmental risks. (Zinatloo-Ajabshir and Zinatloo-Ajabshir, 2019; Allah and Alshamsi, 2023) However, the application of nanotechnology has led to the widespread availability of nanoplastics. Given that polystyrene nanoparticles (PS NPs) constitute a significant category of microplastics, it is crucial to assess their hazardous effects. However, a dearth of sufficient data on the toxicity of PS to environmentally significant species hampers the quantitative evaluation of nanomaterial-associated risks. (Doktorovova et al., 2014; Zielinska et al., 2020) Consequently, urgent attention is required to investigate the hazardous consequences of nanomaterials, particularly focusing on aquatic creatures directly at risk due to their presence.

While previous studies have predominantly focused on the effects of microplastics on mollusks and zebrafish, limited research has been conducted on amphibians. Amphibians, as essential freshwater creatures, face direct exposure to pollutants, rendering them more susceptible to the impact of microplastics. (Hayes et al., 2010; Babini et al., 2016) The bullfrog was chosen as a representative amphibian species for this investigation. (De Arcaute et al., 2014; Cruz-Esquível et al., 2017) Their distinctive aquatic lifestyle and the permeability of their skin during early stages make them prone to direct and continuous exposure to pollutants, making them a suitable choice for exposure experiments involving harmful substances. (Mouchet and Gauthier, 2013)

While numerous acute toxicity tests have indicated negative effects on aquatic organisms, knowledge about the long-term biotoxicity effects of nano-plastics remains limited. (Besseling et al., 2014; Brandts et al., 2018; Zhang et al., 2018) PS NP exposure is an ongoing process, including the continual release of industrial wastewater and the accumulation of PS NPs in ponds. Moreover, the breakdown of PS NPs is a protracted process, and they can remain stable within the body for an extended period. (Najah-Missaoui et al., 2020) Therefore, evaluating the potential long-term danger of PS NPs to tadpoles through subacute toxicity experiments is imperative.

However, the location and mechanisms underlying the risks associated with long-term exposure of amphibian larvae to PS NPs remain unclear. Currently, experimental data on the harm caused by long-term exposure of PS NPs to tadpoles is relatively limited. This experiment aims to investigate how PS NPs affect oxidative stress levels and liver health in tadpoles. Fluorescence microscopy and Py-GC-MS were employed to examine the dispersion and buildup of PS NPs in tadpoles. After 51 days of exposure, pathological sections were taken to detect potential lesions, and transmission microscopy was utilized to observe intracellular damage. The liver's oxidative stress was evaluated by assessing SOD, CAT, GSH, and MDA levels in each group. This research provides a valuable opportunity to gain deeper insights into the influence of PS NPs on tadpole growth.

2. Materials and methods

2.1. Reagents

Orange-red fluorescent PS NPs of sizes 100 nm were obtained from Beijing Jingshi Ruige Technology Co., Ltd. (Beijing, China). DAPI (4',6-diamidino-2-phenylindole) is a lipid-soluble fluorochrome that has a high affinity to DNA and a lower affinity to RNA. (Xing et al., 2015) DAPI Staining Solution was supplied by Xi'an Qiyue Biotechnology Co., Ltd. Superoxide Dismutase (SOD) assay kit (Hydroxylamine method) (SOD; Product n. A001-3-2), GSH assay kit (GSH; Product n. A006 - 2-1) Catalase assay kit (Visible light) (CAT; Product n. A007-1-1) and Plant Malondialdehyde (MDA) assay kit (Colorimetric method) (MDA; Product n. A003-1-2) were supplied by Nanjing Jiancheng Bioengineering Institute, (Nanjing, China). The protein content assay kit

(Coomassie brilliant blue) (Product n. KMSP-1-W) was provided by Comin Biotechnology Co., Ltd. (Suzhou, China).

2.2. Preparation and characterization of Polystyrene nanospheres

Initially, 267 ml of distilled water was introduced into a flask and subjected to a water bath at 80°C, with a continuous flow of N2 for approximately 10 minutes. Subsequently, a mixture of 1 ml of methacrylic acid and 10 ml of styrene was prepared. A combination of 0.15 g of potassium persulfate with 3 ml of water was gradually introduced after 30 minutes. The nitrogen was then purged through a venting process for about 50 minutes, followed by removal through stirring in the water bath for approximately 12 hours.

For the examination of the polystyrene (PS) morphology, transmission electron microscopy (TEM; Hitachi H-7650, Tokyo, Japan) with a 120 kV accelerating voltage and scanning electron microscopy (SEM) were employed. Particle size distribution and zeta potential in the exposure solutions were assessed using the Zetasizer Nano ZS (ZEN 3600, Malvern, U.K.). Notably, no precipitate was observed in the spiked water even after three days, indicating the stability of PS NPs.

In the experimental procedure, ultrasonic treatment was conducted 30 minutes before application to ensure the full dispersion of nanoplastics in the suspension. Subsequently, the nano-plastic suspensions were introduced into the corresponding experimental tank and uniformly distributed in the water through aeration.

2.3. Animals maintenance

Tadpoles (*R. limnochari*) at developmental stages GS12-GS18 were procured in Shantou, Guangdong, China, between May and July 2023. Subsequently, adhering to a density of 16 tadpoles per liter, these specimens were transferred to an aquarium measuring 20×20×15 cm. Throughout the experiment, the tadpoles were reared in aquaria filled with dechlorinated tap water (pH 6.9–7.1) at a temperature of 22°C ± 2°C, maintaining a dissolved oxygen concentration of 7.0 ± 0.1 mg/L. The photoperiod was standardized at 12:12 light: dark. Commercial food manufactured by Hongyi Feed Co., Ltd (Guangdong, China) was provided to the tadpoles. Ultimately, the water bath was turned off, and the system was left undisturbed for an additional 12 hours. Half of the water in the tank was replaced every two days to stabilize the pH, and the tadpoles were also ensured to be fed every day. All these procedures in the present study were approved by the Animal Ethics Committee of China Agricultural University.

2.4. Uptake and distribution of PS NPs

Following 24 hours of fasting, tadpoles were randomly distributed into 3 glass tanks, each accommodating nine tadpoles. The experimental group was exposed to fluorescent polystyrene nanoparticles (PS NPs) with a diameter of 100 nm and added to the culture water to achieve a final concentration of 100 µg/L. Sampling was conducted at three distinct time points: 24 h, 48 h, and 72 h, with three tadpoles utilized for each time point. The animals were anesthetized with lidocaine and euthanized. Tadpoles from both the group treated with 100 µg/L fluorescent PS NPs and the control group were preserved at –80°C, embedded in optimum cutting temperature compound (O.C.T.) (Shanghai Solar Bioscience & Technology Co., LTD), sectioned at a thickness of 5 µm and stained with DAPI for microscopic analysis. To ascertain the ingestion and distribution of particles, a fluorescence microscope (Zeiss Axio Imager A1) was employed to examine the presence of PS NPs (fluorescing orange-red) within the gills, liver, and gut of the tadpoles.

2.5. Toxicity experimental design

Tadpoles were randomly assigned to control and polystyrene

nanoparticles (PS NPs) treatment groups, with PS NPs exposure concentrations mimicking levels of environmental pollution. (Egessa et al., 2020; Kai et al., 2017; Xiong et al., 2019; shiye et al., 2021; Xiong et al., 2018). The animals were divided into four treatments with three repetitions each. The groups were exposed to 100 nm virgin PS NPs at concentrations of 0 µg/ml (Group A), 10 µg/ml (Group B), 40 µg/ml (Group C), and 80 µg/ml (Group D). Each PS NP concentration was subjected to histopathological analysis and oxidative stress analysis using 156 tadpoles. These tadpoles were randomly distributed into twelve tanks, with eight tadpoles in each tank. Three tanks were allocated to each treatment group (exposed to 10, 40, or 80 µg/L PS NPs) and the control group (culture water without particles). Additionally, 60 tadpoles were designated for transmission electron microscopy (TEM) analysis. These tadpoles were randomly placed into 12 tanks, with five tadpoles in each tank. Three tanks were assigned to each treatment group and the control group, and they were exposed for 51 days.

The preparation of the test solution and tadpole maintenance mirrored the procedures mentioned earlier. Following exposure, tadpoles were carefully rinsed on a steel grid to eliminate any PS NPs from their skin. Each tadpole was then dissected, promptly frozen in liquid nitrogen, and stored at -80 °C for oxidative stress analysis or fixed in 10% formalin for histopathological examination. The two groups of tadpoles were with three repetitions each. All these procedures in the present study were approved by the Animal Ethics Committee of China Agricultural University.

2.6. Analysis by Py-GC/MS

Following a 51-day exposure period, tadpoles were deliberately starved to minimize gut contents and euthanized after anesthesia in a sterile environment. One tadpole from each group was chosen, thoroughly rinsed to remove surface-bound PS NPs, and subsequently pulverized using a grinder.

Place approximately 1 g of the sample (equivalent to a thousand pounds) into a 20 ml container. Directly pour around 5 ml of trichloromethane solution into the specimen container. The combined solution with the samples underwent sonication for 10 minutes, followed by the extraction and filtration of the supernatant using filter paper to isolate the soluble substance. Keep incorporating a blend of trichloromethane and tetrahydrofuran into the sample container for polystyrene extraction. Repeat these steps three times.

Standards with varying concentrations were prepared and subjected to Pyrolysis-Gas Chromatography-Mass Spectrometry (Py-GCMS) for testing, enabling the construction of a quantitative curve. A portion of the tadpole sample was concentrated, and post-concentration, it was carefully added drop by drop into the injection crucible of the Py-GCMS using a glass pipette. Following the complete evaporation of the solvent in the crucible, the sample was analyzed by Py-GCMS (GC-MS model: GCMS-QP2020; pyrolyzer: PY-3030D F).

2.7. Histopathological analysis

Tadpoles were chosen at random from each group (one tadpole per tank), euthanized under anesthesia in a sterile setting, and dissected to extract the liver. The liver was subsequently immersed in a 4% Poly-formaldehyde (PFA) solution overnight. It was then subjected to a series of processes, including washing, dehydration using a gradient concentration of C2H5OH and C8H10 transparent, embedding in paraffin, sectioning at a thickness of 5 µm, and finally staining with haematoxylin-eosin (H&E) for microscopic analysis.

2.8. Oxidative stress analysis

To assess the oxidative stress induced by polystyrene nanoparticles (PS NPs) in tadpoles, the activities of superoxide dismutase (SOD) and catalase (CAT), along with the concentrations of malondialdehyde

(MDA) and glutathione (GSH) in the livers of tadpoles, were determined. For each replicate, the livers of four tadpoles were combined to form one sample, and 60 mg of homogenized tissue was utilized for analysis. To minimize the impact of individual variability on the studied traits, liver samples of four individuals were washed with sterile phosphate-buffered saline (PBS) and pooled in a 2 ml RNase/DNase-free cryogenic vial (Corning, 430,659-ND). The pooled liver samples were shock-frozen in liquid nitrogen and stored at -80 °C before biochemical analysis.

The liver of juvenile fish was homogenized (1:9 w/v) in ice-cold physiological saline solution with 0.89% buffer. Commercial kits from Jiancheng Bioengineering Institute, Nanjing, China, were employed to measure the levels of SOD, CAT, MDA, and GSH. The activities of SOD and CAT were measured based on the colorimetric method. The contents of MDA were detected as the levels of the thiobarbituric acid-reactive substances. Protein content was quantified using bovine serum albumin as a standard. All assay protocols and calculations of enzyme activities or MDA concentrations were based on the manufacturer's instructions. Each assay was performed in triplicate.

2.9. Biological transmission electron microscope (TEM) observation

Fresh liver tissues were cut into pieces measuring 2–3 mm³ and promptly submerged in a pre-cooled 2.5% glutaraldehyde fixative at 4 °C. To ensure proper fixation, gas from the tissues was withdrawn using a syringe, allowing them to sink into the fixative. Subsequently, the tissues were fixed overnight at 4 °C. The preparation of section samples and biological transmission electron microscopy (TEM) analysis were conducted using a Leica Artos 3D ultra-thin microtome and a Hitachi HT7800 TEM.

2.10. Statistical analysis

The results were expressed as mean ± standard deviation (SD). One-way analysis of variance (ANOVA) was used to evaluate the statistical differences between the biological parameters of the control and treatment groups. All of the analyses were performed using GraphPad Prism 8 software. A p-value of <0.05 was accepted as indicating significance.

3. Result

3.1. Characterization of PS NPs

To investigate the toxicity of polystyrene nanoparticles (PS NPs), nanoparticles were synthesized in the laboratory using a one-pot method. Scanning electron microscopy and transmission electron microscopy revealed that the PS NPs exhibited uniform spherical shapes with an average diameter of 150 nm, evenly dispersed throughout the field of vision (Fig. 1a-d).

Fig. 1e illustrates the characteristics of the synthesized nanoparticles in double distilled water, as measured by Zetasizer Ver 7.02. The hydrodynamic size of the PS NPs averaged 165 nm, displaying a narrow size distribution, as evidenced by a polymer dispersity index of 0.027. The zeta potential of PS NPs was determined to be -35.6 mV. The Fourier-transform infrared (FTIR) detection data of the synthesized PS NPs, analyzed using the software OMNIC for spectral analysis, confirmed that the main absorption peak aligned with the peak characteristics of polystyrene. Based on this comprehensive material characterization, it is affirmed that 100 nm PS NPs have been successfully synthesized.

3.2. Accumulation and distribution of PS NPs in tadpole tissues

Plastic content (µg/g microplastic mass/tadpole weight) in tadpoles in each group was detected by Py-GCMS. (Fig. 1f) In the control group, the concentration of PS NPs was minimal, whereas groups B to D had concentrations of 8.298 µg/g, 11.74 µg/g, and 12.03 µg/g. It can be

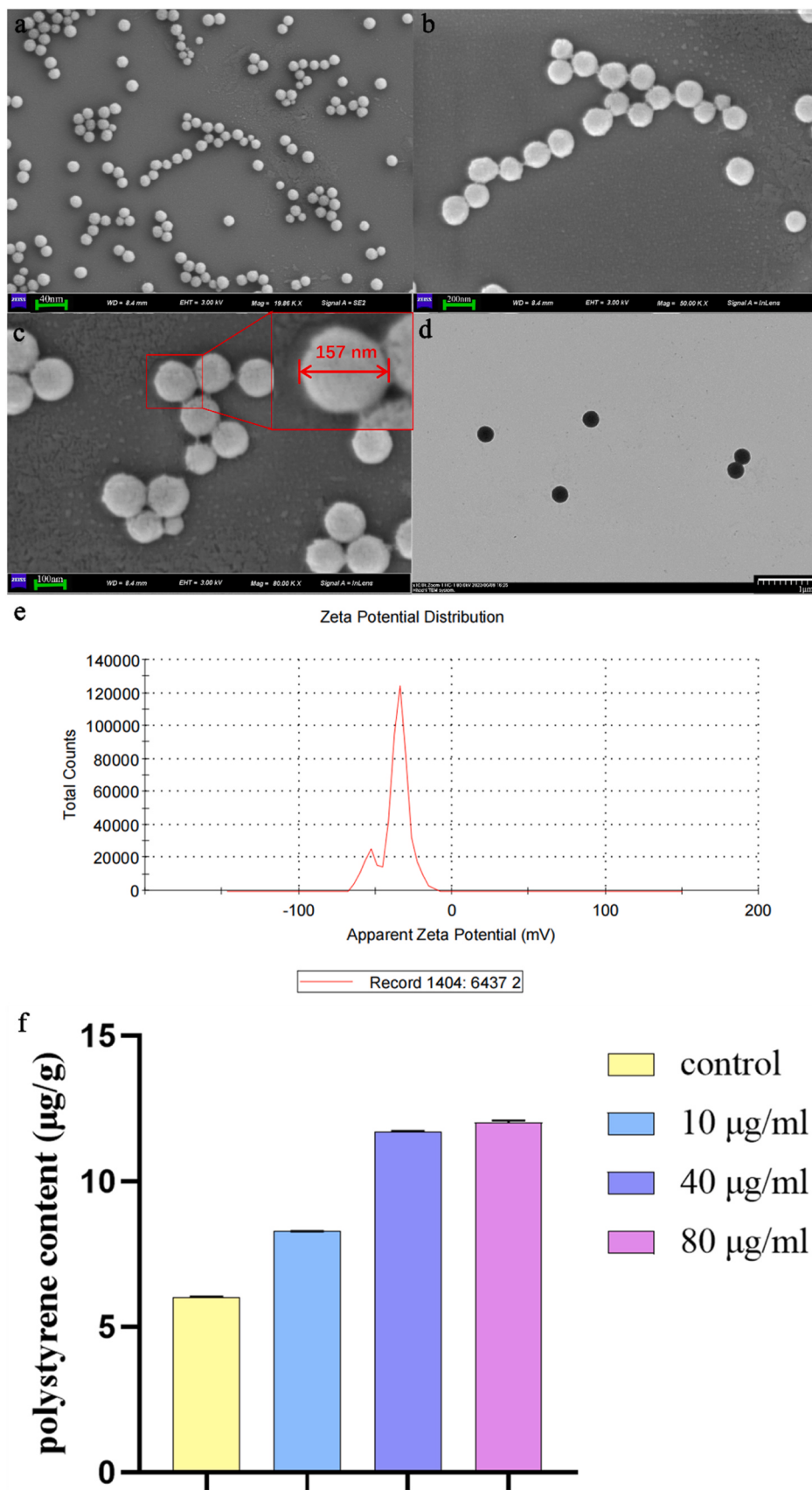


Fig. 1. a-c) The SEM image of PS NPs. d) The TEM image of PS NPs. e) Zeta potential f) Polystyrene content in tadpoles (expressed in $\mu\text{g/g}$ dry weight).

inferred that the tadpoles' PS NP levels increase in proportion to the concentration of exposure.

After being exposed to nanoparticles, fluorescence was observed in the gills and intestines of tadpoles. Fluorescence microscopy reveals that the fluorescent PS NPs exhibit consistent orange-red particles, while the tadpoles lack their fluorescence. The first column displays the DAPI staining of tadpole gills and intestines, while the second column exhibits the distribution of fluorescent nanomaterials in tadpoles, and the last column synthesizes the DAPI staining map alongside the fluorescence distribution map. In Group A (0 µg/ml) (Fig. 2a and b), fluorescent PS NPs were distributed in gills (Figs. 2a1–3) and intestine (Figs. 2b1–3). In Groups B (Figs. 2c1–3) and C (Figs. 2d1–3), fluorescence was found only in the intestine, and the intensity of fluorescence gradually diminished.

3.3. Histopathological changes induced by treatment with PS NPs

3.3.1. Liver histological analysis

The liver, as a crucial organ for detoxification, displayed a normal tissue structure in tadpoles of the control group (Group A), where all cell types were precisely and tightly arranged (Fig. 3). The hepatic cord exhibited an orderly arrangement (red arrow in Fig. 3b), suggesting the relative health of the tadpoles. Hepatocytes featured larger nuclei with pink cytoplasm, maintaining an intact structure (black arrow in Fig. 3b). Reticular-shaped hepatic sinusoids between the liver plates contained scattered Kupffer cells (blue arrow in Fig. 3b).

Contrastingly, liver damage was observed in Group D (80 µg/ml) (Fig. 3). The sinusoid space underwent dilation and hyperemia (yellow arrow in Fig. 3c), accompanied by the presence of inflammatory cells (blue arrow in Fig. 3e). The liver displayed significant yellowish-brown

deposits, believed to be bile pigment (orange arrow in Fig. 3d). The arrangement of hepatocytes was loose, and the hepatic cord exhibited disorder (purple arrow in Fig. 3e). Hepatocytes showed extensive disappearance of cytoplasm, marked by cell vacuolization (green arrow in Fig. 3e), and nuclear necrosis (black arrow in Fig. 3e). Numerous lobulated punctate nuclei (red arrow in Fig. 3f) were observed in hepatocytes, either encircled by tubes or existing in isolation.

In Group C (40 µg/ml), some bile pigment was also observed, and the blue arrow indicates a decrease in hepatocytes and an increase in leukocytes. For Group B (10 µg/ml), no significant difference from the control group (Group A) was noted. Collectively, these results indicate that pathological alterations in the tadpole liver occurred after exposure to PS NPs.

3.3.2. Kidney histological analysis

The kidney displayed a typical normal structure of the cortex and medulla in microscopical examinations of the control tadpoles. The cortex featured numerous glomeruli with dense blood capillaries.

Histological sections of the kidneys from PS NP-treated groups are presented in Fig. 4. In Group D (80 µg/ml), the kidney exhibited proximal and distal tubular necrosis with variable degrees of stainability. Necrotic cells fell into the tubules' lumen, obliterating them (black arrow in Fig. 4b), and thrombus formation was evident (red arrow in Fig. 4b). Additionally, the renal tubular lumen contained a substantial quantity of pink-staining substance (orange arrow in Fig. 4b). The necrotic area of the renal tubules showed a significant increase in compensatory proliferation (yellow arrow in Fig. 4c). Damage to glomeruli was also noted, including swelling and thickening of cells within the renal capsule wall layer (green arrow in Fig. 4c). Glomerular

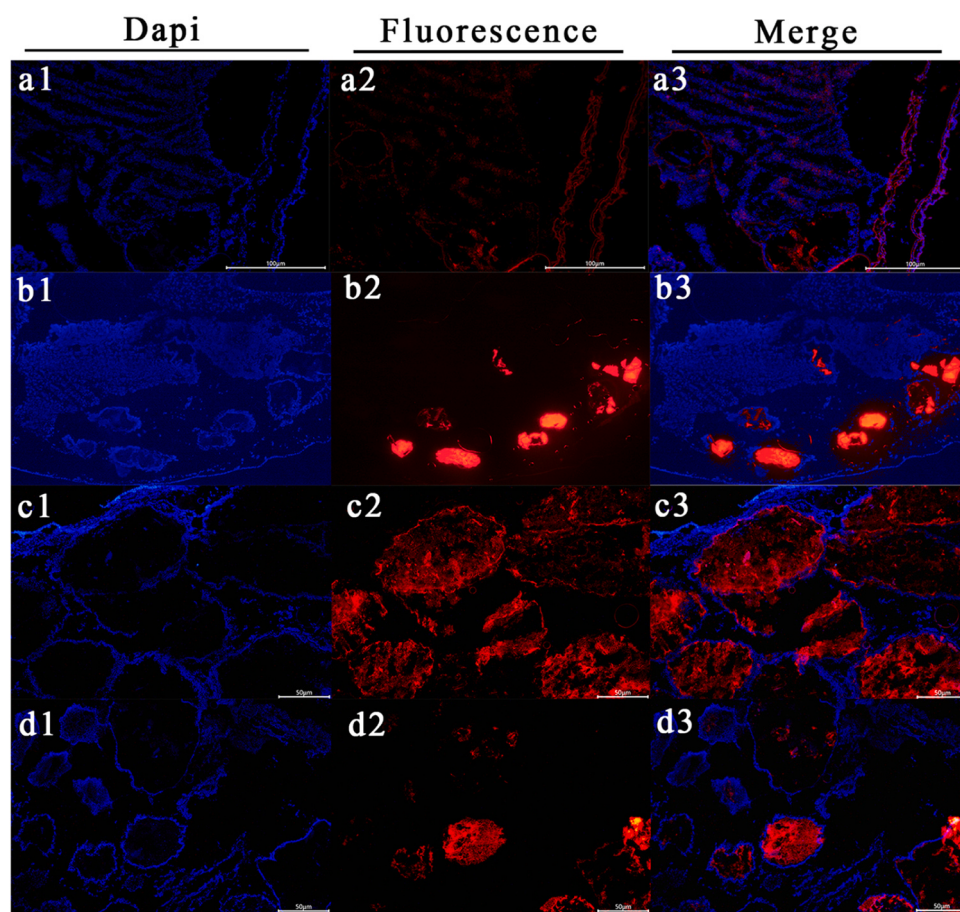


Fig. 2. Enrichment of PS in tadpole. a1-3) Gill in tadpole exposed for 24 h. b1-3) Intestine in tadpole exposed for 24 h. c1-3) Intestine in tadpole exposed for 48 h. d1-3) Intestine in tadpole exposed for 48 h;

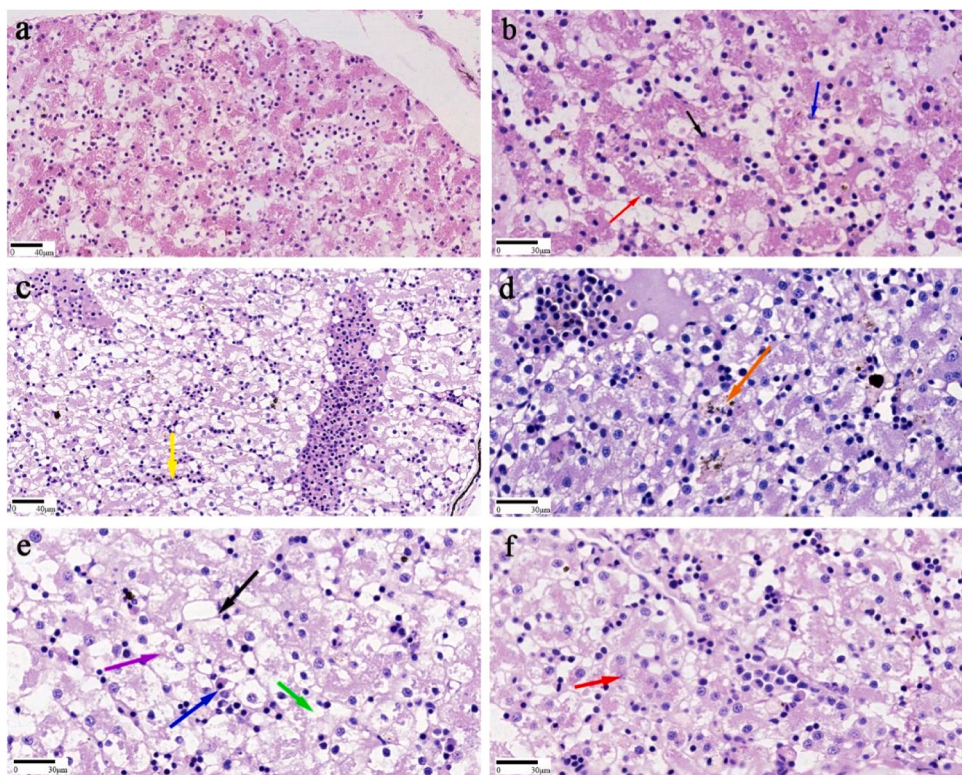


Fig. 3. Damage of PS on the liver in tadpole. H&E stain, the bar size was indicated under pictures. a, b) Tadpole from the control group (Group A). The hepatic cord was arranged orderly (red arrow), and the structure of hepatocytes was intact (black arrow). The hepatic sinusoids between the liver plates are reticular in shape (blue arrow). c-f) Liver in tadpole exposed at a concentration of 80 µg/ml (Group D). The sinusoid space experienced dilation and hyperemia (yellow arrow, a). The liver exhibited significant bile pigment deposits (orange arrow, b). The hepatic cord was arranged in disorder (purple arrow, c). The cytoplasm of hepatocytes disappeared in large quantities, with cell vacuolization (green arrow, c), nuclear necrosis (black arrow, c), and inflammatory cell infiltration (blue arrow, c). Numerous lobulated punctate nuclei (red arrow, d) could be seen in hepatocytes.

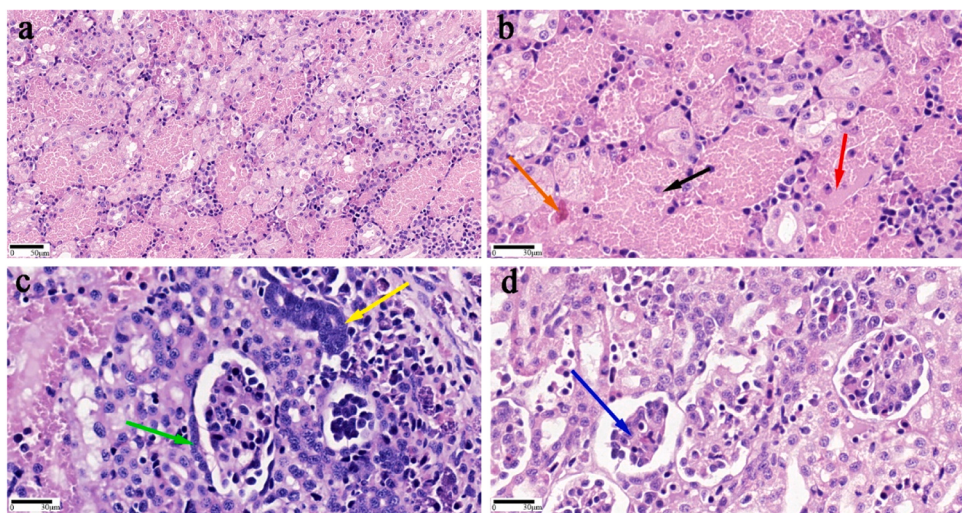


Fig. 4. Damage of PS on the kidney in tadpole. a-d) Kidney in tadpole exposed at a concentration of 80 µg/ml (Group D). H&E stain, the bar size was indicated under pictures.

atrophy (blue arrow in Fig. 4d) was observed, with severe cases forming scattered red staining.

Tadpoles from Group C (40 µg/ml) exhibited dilation of capillaries in the glomerulus, with white blood cells found between the capillary networks.

The necrotic cells fell into the tubules' lumen (black arrow, b). The renal tubular lumen was filled with a pink staining substance (orange arrow, b) and there was a thrombus present (red arrow). The necrotic

area of the renal tubules experiences a significant increase in compensatory proliferation. (yellow arrow, c) Swelling and thickening of the cells (green arrow, c) within the renal capsule wall layer were observed. The glomeruli atrophy and necrosis (blue arrow, d).

3.4. Oxidative stress induced by treatment with PS NPs

This study investigated the oxidative stress induced by PS NPs

treatment in tadpoles' livers by evaluating the activities of superoxide dismutase (SOD) and catalase (CAT), as well as the content of glutathione (GSH) and malondialdehyde (MDA) (Fig. 5). In Group D (80 µg/ml), a robust oxidative stress response, as evidenced by decreased activities of SOD and CAT, along with heightened GSH levels, was observed in the tadpoles' liver. Simultaneously, the presence of Group C (40 µg/ml) resulted in a decline in CAT activities and a substantial rise in GSH levels. However, Group B (10 µg/ml) did not lead to any noteworthy variation in these crucial indicators. Elevated levels of lipid peroxidation, indicated by MDA, were only found in the liver of tadpoles in Group D (80 µg/ml).

3.5. Biological TEM analysis

The nuclei exhibited typical nuclear membranes (NM) with scattered heterochromatin clusters. The cytoplasm exhibited a high level of electronic density and uniformity, with readily discernible parallel rough endoplasmic reticulum (RER) (Fig. 6a and b). The nucleus and mitochondria in endothelial cells were structurally intact (Fig. 6c). The cytoplasm of fat-storing cells contained round or ovoid double-membraned mitochondria (M) with visible ridges (Fig. 6d).

Fig. 7 illustrates an increase in the presence of black bead-like particles of foreign matter within the hepatocytes following exposure in Group D (80 µg/ml). The edges of these particles exhibited clarity and uniformity, devoid of any apparent integration with adjacent tissues, and their dimensions were approximately 100 nm, echoing the size of the PS NPs used in exposure experiments (Fig. 1d). Tissues containing nanoparticles exhibited pronounced nuclear necrosis of hepatocytes

(Fig. 7b). The nuclei of the cells depicted in the figure underwent a significant reduction in size and an intensification in color, resulting in pronounced pyknosis (Fig. 7a). Simultaneously, there was a decrease in cytoplasmic density, indicating cellular swelling. The particle content within the Kupffer cells was higher than that of the hepatocytes and endothelial cells (Fig. 7d and e). At the same time, a large number of apoptotic vesicles could be observed in the cytoplasm. The apoptotic vesicles were round and low-density, phagocytosing the mitochondria. The double-layer membrane structure of mitochondria was abnormal, and the cell underwent disintegration and death (Fig. 7f).

Group C (40 µg/ml) exhibited a reduced presence of particles, and the cells displayed a diminished number of lesions. Nevertheless, a faint condensation of the nucleoli and a partially irregular nuclear membrane could still be observed. No noteworthy lesions were detected in Group B (10 µg/ml).

4. Discussion

The article bridges the gap between the hazards that amphibians suffer from prolonged exposure to polystyrene nanoparticles. The findings from Py-GCMS indicated that PS NPs accumulate in tadpoles, with levels increasing in proportion to the exposure dose. This accumulation was also found in *Paphia undulata*. (Kang et al., 2023) The accumulation of microplastics in tadpoles indicates potential buildup, with even the control group exhibiting unexpectedly levels of PS NPs, possibly from prior exposure to water with elevated microplastic concentrations.

The distribution of 100 nm polystyrene nano microspheres was observed in the gills, intestinal lumen, and liver of tadpoles. In this

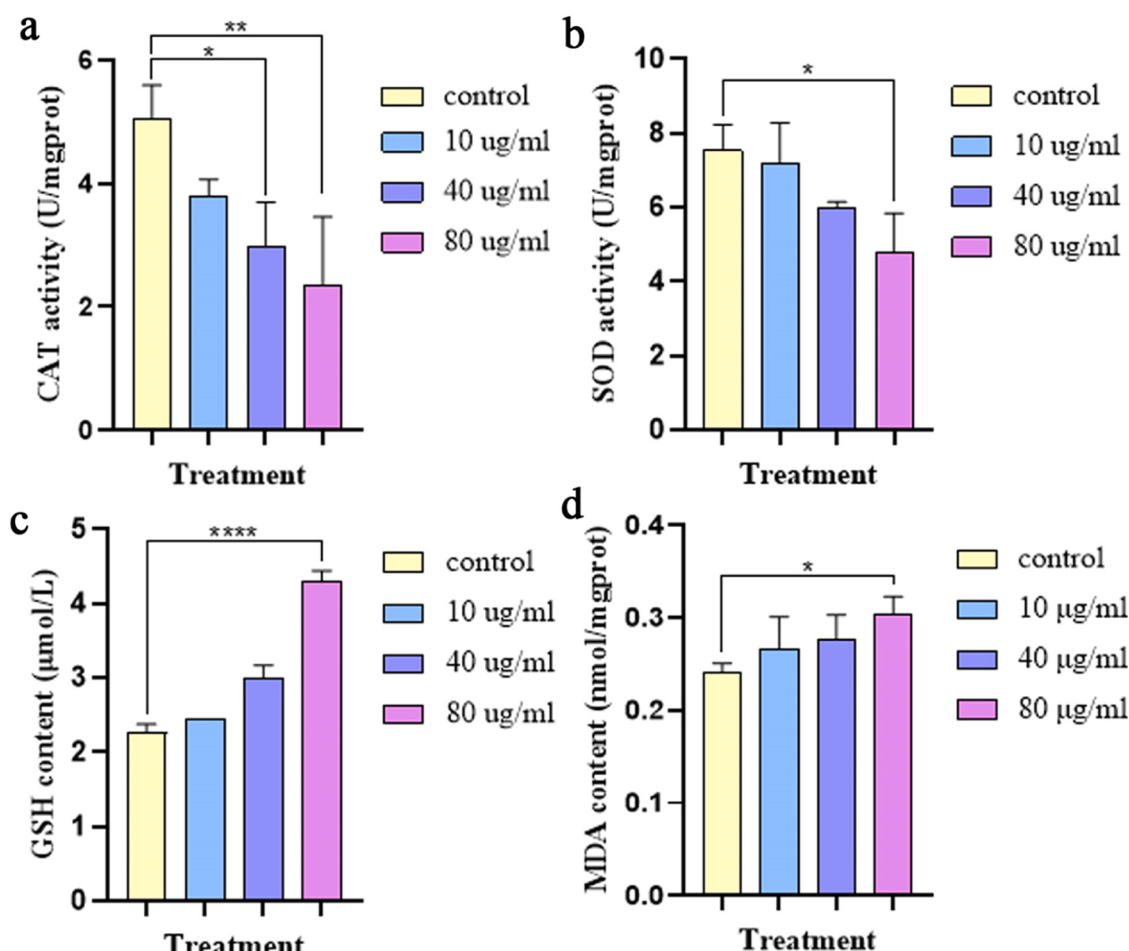


Fig. 5. Antioxidants of tadpole exposed to three concentrations of PS. a) CAT. b) SOD. c) GSH. d) MDA. Error bars indicate mean ± standard deviation ($n = 3$). Significant differences were analyzed by one-way ANOVA (Tukey post hoc test). *, $P < 0.05$; **, $P < 0.01$; ***, $P < 0.001$, ****, $P < 0.0001$.

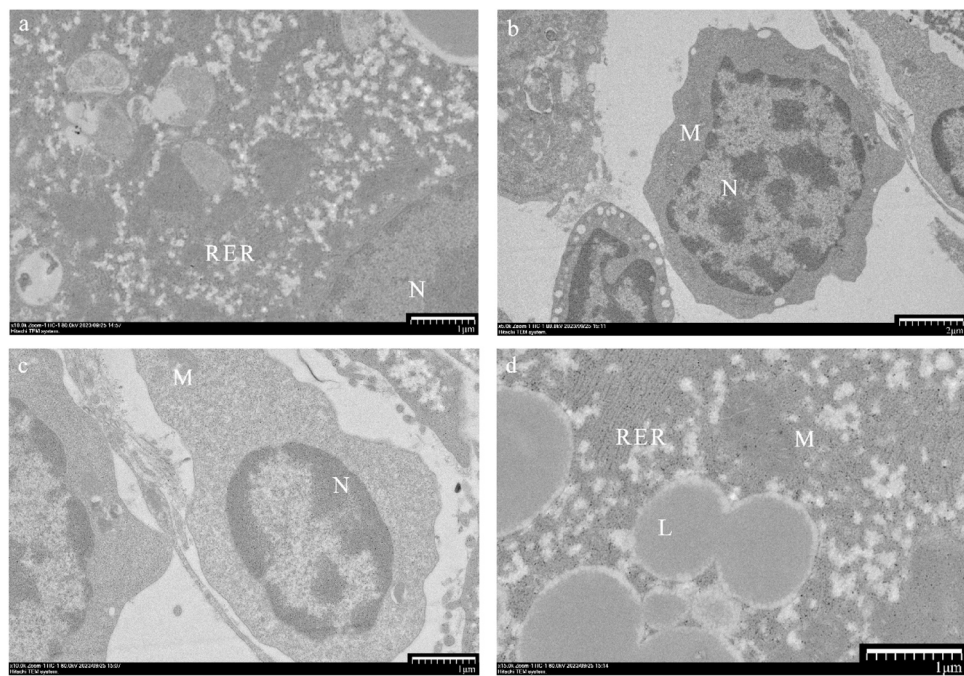


Fig. 6. Electron microscopic picture of hepatocytes from tadpole in the control group. a) Hepatocyte b) Kupffer cell c) Endothelial cell d) fat-storing cell. L: Lipid; M: Mitochondrion; N: Nucleus; PS: Polystyrene nanoparticles; RER: Rough endoplasmic reticulum;

study, the accumulation of microspheres in tadpoles exhibited a time-dependent relationship. These findings align with similar accumulation patterns observed in sea urchin larvae (*Tripneustes gratilla*) and crabs. (Kaposi et al., 2014; Farrell and Nelson, 2013; Hu et al., 2016) However, certain studies have indicated a time-independent correlation in the accumulation of microspheres within tadpoles (Rosenkranz et al., 2009; von Moos et al., 2012). One hypothesis suggests that the reduced fluorescent intensity in the clustered fluorescent particles may be associated with their varying sizes (Abarghouei et al., 2021). Similar distribution patterns have been reported in other aquatic organisms like zebrafish and crabs. (Watts et al., 2014; Lu et al., 2016a). The longer-lasting and more pronounced fluorescence in the intestine compared to the gills may be attributed to the intestine's superior capacity for accumulation and absorption. (Lacave et al., 2018)

The presence of black, uniformly shaped particles was observed in the liver tissue by TEM. Additional studies have demonstrated that nanoparticles are capable of penetrating the liver, leading to liver harm. (Lee et al., 2013; Bartucci et al., 2020; Li et al., 2022; Habumugisha et al., 2023; Jia et al., 2024) The black bead-like particles measure approximately 100 nm in size, aligning with the PS NPs utilized in the characterization. This serves as proof that plastic nanomaterials can penetrate these liver tissues, implying that the liver plays a crucial role in nanoparticle processing. (Migwi et al., 2020) The liver's accumulation of nanoparticles may be due to it being the main detoxification organ. (Decuzzi et al., 2010; Sharma et al., 2012; Lacave et al., 2018)

The experimental groups exhibited a great degree of hepatic dilatation and congestion. In Group D (80 µg/ml), a substantial accumulation of bile pigments was observed irregularly. Typically, hepatocytes generate bile pigments which are subsequently via the biliary system entering the duodenum. The existence of substantial quantities of bile pigments suggests a disruption in certain aspects of the aforementioned procedure. (Kullak-Ublick and Meier, 2000) The presence of numerous inflammatory cells implies that the immune system may cause harm to bile canalculus epithelial cells, resulting in bile seepage. (Lazaridis and Larusso, 2015) Necrosis is caused by toxic substances that specifically attack organelles, resulting in detrimental effects on mitochondria and the endoplasmic reticulum. (Almansour et al., 2017)

The data indicate that the detrimental effects caused by PS-NPs may

be linked to the mechanism of oxidative stress. Increased MDA levels have been consistently observed in comparable studies (Yasin et al., 2022; Du et al., 2024). While some research suggests a decline in SOD and CAT levels with greater concentrations (Jia et al., 2024; Zaman et al., 2024), other studies demonstrate an elevation in both parameters, coupled with a decline in GSH content. (Li et al., 2020; Estrela et al., 2021). It is worth mentioning, however, that the duration of exposure to hazardous substances in the aforementioned experimental studies was significantly shorter compared to the growth cycle of the experimental animals. A briefer period of activity does not impede enzyme activity, but instead stimulates the entire antioxidant system, resulting in an upsurge in SOD and CAT activity. (Huang et al., 2020) Likewise, during the initial phases of ROS elimination, GSH undergoes significant depletion, leading to a decline in its concentration. To put it succinctly, the discrepancies in findings are largely dependent on the duration of the experiment.

Superoxide dismutase (SOD) and catalase (CAT) play a crucial role as antioxidant enzymes. The SOD system is often seen as the initial defense mechanism for the production of reactive oxygen species (ROS) in the face of environmental pressures (Pandey et al., 2003), and in the battle against oxidative stress, a great deal of energy is used up, leading to a decrease in enzyme production and activity. (Kim et al., 2021)

The decrease in SOD activity may be due to the continuous production of ROS in chronic toxic environments, resulting in a decrease in the activities of antioxidant enzymes. (Xia et al., 2020) Moreover, as a consequence of the prolonged exposure, PS NPs caused a total deterioration in the antioxidant capacity. (Yang et al., 2020) Numerous investigations have been consistently carried out regarding the results of CAT. The presence of PS NPs caused an imbalance in the antioxidant system (Xia et al., 2020) and the inhibition of antioxidant enzymes. (Clasen et al., 2018) Glutathione plays a crucial role in maintaining redox balance as a non-enzymatic antioxidant system. The breakdown of enzymatic antioxidant systems triggers the activation of glutathione-dependent antioxidant systems, subsequently exerting a substantial compensatory by elevating GSH levels. (Wen et al., 2018) Malondialdehyde (MDA) can be used as a marker to measure lipid peroxidation (LPO), which is the result of oxidative damage to lipids. (Alomar et al., 2017) The disturbance of the antioxidant system initiates

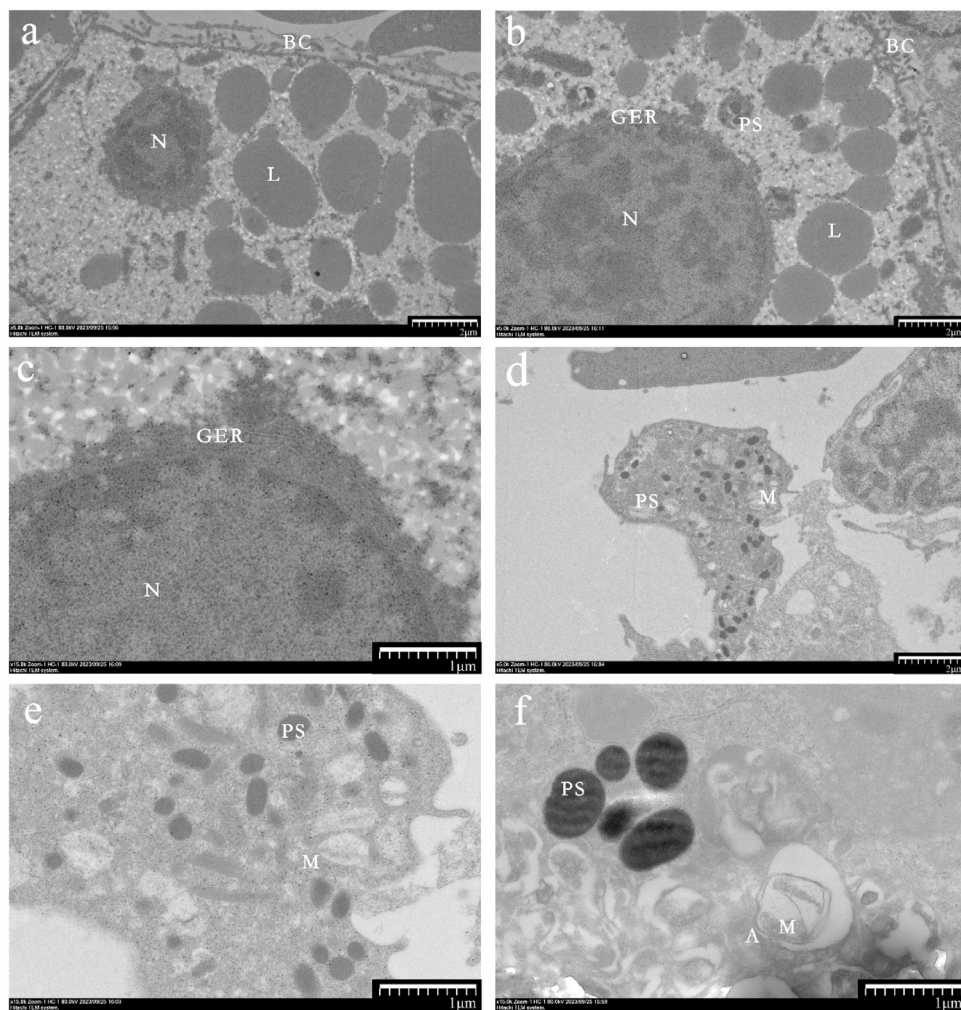


Fig. 7. Electron microscopic picture of hepatocytes from tadpole exposed at a concentration of 80 µg/ml. a-c) Hepatocyte d-f) Kupffer cell. A: Autophagosome; BC: Bile canalculus; L: Lipid; M: Mitochondrion; N: Nucleus; PS: Polystyrene nanoparticles; RER: Rough endoplasmic reticulum;

the assault of free radicals on the lipid membrane, leading to an elevation in MDA levels. This indicates an increased degree of oxidative stress. (Wang et al., 2019)

Using electron microscopy, nanoparticles show potential bioaccumulation in various organs and physiological changes at the ultrastructural level. Nuclear pyknosis, indicating severe and irreversible liver damage, is observed as irreversible chromatin condensation in the nucleus. (Attia et al., 2021) The organelles suffer the most severe damage to their mitochondria. High doses of medication can cause serious damage to mitochondria, which may be linked to toxic substances and hormonal imbalances. (Bizjak Mali et al., 2013; Ansari et al., 2016) The impairment of the mitochondria can lead to inadequate energy generation, impacting the production of proteins in the rough endoplasmic reticulum, including apolipoproteins, and potentially resulting in cellular harm. (Fishelson, 2006; Ozturk et al., 2009)

Currently, freshwater is rich in nanoparticles, posing direct risks to amphibians who encounter these substances. The significance of this document lies in its role in preserving wild amphibians and maintaining human health.

5. Conclusion

In summary, the study concludes that polystyrene nanoparticles (PS NPs) induce liver damage in tadpoles, primarily by elevating oxidative stress levels. The accumulation of polystyrene nanoparticles in tadpoles has been demonstrated, with the intestines and gills being their primary

sites of accumulation. These nanoparticles are capable of penetrating the liver and accumulating in Kupffer cells and hepatocytes. Prolonged exposure to polystyrene nanoparticles can induce pathological damage to the tadpole's liver and kidneys, with more pronounced effects on the liver. Examination of the liver's submicroscopic structure revealed severe hepatocyte necrosis and significant mitochondrial damage. Assessment of oxidative stress markers including SOD, CAT, GSH, and MDA showed disrupted antioxidant levels and increased oxidative products, indicating that polystyrene nanoparticles pose harm to tadpoles by affecting hepatic oxidative status. This study focuses on the long-term effects of polystyrene nanoparticles on amphibian larvae, filling a gap in related research. These findings provide valuable insights for assessing the toxicity of polystyrene nanoparticles.

CRediT authorship contribution statement

Cenxi Zhao: Writing – review & editing, Visualization, Methodology, Data curation. **Xuepeng Teng:** Conceptualization, Writing – review & editing. **Hao Zang:** Writing – review & editing, Writing – original draft, Visualization, Project administration, Methodology, Investigation, Conceptualization. **Chaoyu Zhou:** Writing – review & editing, Investigation. **Liutao Wei:** Visualization, Methodology. **Tianlong Liu:** Conceptualization, Project administration, Supervision. **Jie Chai:** Data curation. **Haiyan Wu:** Methodology, Data curation. **Runqiu Cai:** Investigation, Data curation.

Declaration of Competing Interest

The authors declare that they have no known competing financial interests or personal relationships that could have appeared to influence the work reported in this paper.

Data availability

No data was used for the research described in the article.

Acknowledgment

Natural Science Foundation of Shandong Province (Natural Science Foundation of Shandong), Grant/Award Number: ZR2021MH108.

Appendix A. Supporting information

Supplementary data associated with this article can be found in the online version at doi:10.1016/j.ecoenv.2024.116331.

References

2014. Kaposi K.L., MOS B, KELAHER B P, et al. 2014. Ingestion of microplastic has limited impact on a marine larva. *Environ Sci Technol* [J], 48: 1638–1645..
- Abarghouei, S., Hedayati, A., Raeisi, M., et al., 2021. Size-dependent effects of microplastic on uptake, immune system, related gene expression and histopathology of goldfish (*Carassius auratus*). *Chemosphere* [J.] 276.
- Allah, M., Alshamsi, H.A., 2023. Green synthesis of AC/ZnO nanocomposites for adsorptive removal of organic dyes from aqueous solution. *Inorg. Chem. Commun.* [J.] 157.
- Almansour, M.I., Alferah, M.A., Shraideh, Z.A., et al., 2017. Zinc oxide nanoparticles hepatotoxicity: Histological and histochemical study. *Environ. Toxicol. Pharmacol.* [J.] 51, 124–130.
- Alomar, C., Sureda, A., Capó, X., et al., 2017. Microplastic ingestion by *Mullus surmuletus* Linnaeus, 1758 fish and its potential for causing oxidative stress. *Environ. Res.* [J.] 159, 135–142.
- Ansari, M.A., Shukla, A.K., Oves, M., et al., 2016. Electron microscopic ultrastructural study on the toxicological effects of AgNPs on the liver, kidney and spleen tissues of albino mice. *Environ. Toxicol. Pharmacol.* [J.] 44, 30–43.
- Aragaw, T.A., 2020. Surgical face masks as a potential source for microplastic pollution in the COVID-19 scenario. *Mar. Pollut. Bull.* [J.] 159, 111517.
- Attia, A.A., Ramdan, H.S., Al-Eisa, R.A., et al., 2021. Effect of saffron extract on the hepatotoxicity induced by copper nanoparticles in male mice. *Mol.* [J.] 26.
- Babini, M.S., Bionda, C.D.E.L., Salas, N.E., et al., 2016. Adverse effect of agroecosystem pond water on biological endpoints of common toad (*Rhinella arenarum*) tadpoles. *Environ. Monit. Assess.* [J.] 188, 459.
- Bartucci, R., Åberg, C., Melgert, B.N., et al., 2020. Time-resolved quantification of nanoparticle uptake, distribution, and impact in precision-cut liver slices. *SMALL* [J.] 16.
- Besseling, E., Wang, B., Lürling, M., et al., 2014. Nanoplastic Affects Growth of *S. obliquus* and Reproduction of *D. magna*. *Environ. Sci. Technol.* [J.] 48, 12336–12343.
- Bizjak Mali, L., Sepčić, K., Bulog, B., 2013. Long-term starvation in cave salamander affects on liver ultrastructure and energy reserve mobilization. *J. Morphol.* [J.] 274, 887–900.
- Brandts, I., Teles, M., Gonçalves, A.P., et al., 2018. Effects of nanoplastics on *Mytilus galloprovincialis* after individual and combined exposure with carbamazepine. *Sci. Total Environ.* [J.] 643, 775–784.
- Clasen, B., Loro, V.L., Murussi, C.R., et al., 2018. Bioaccumulation and oxidative stress caused by pesticides in *Cyprinus carpio* reared in a rice-fish system. *Sci. Total Environ.* [J.] 626, 737–743.
- Cruz-Esquível, Á., Viloria-Rivas, J., Marrugo-Negrete, J., 2017. Genetic damage in *Rhinella marina* populations in habitats affected by agriculture in the middle region of the Sinú River, Colombia. *Environ. Sci. Pollut. Res Int* [J.] 24, 27392–27401.
- Cui, R., Kim, S.W., An, Y.J., 2017. Polystyrene nanoplastics inhibit reproduction and induce abnormal embryonic development in the freshwater crustacean *Daphnia galeata*. *Sci. Rep.* [J.] 7, 12095.
- De Arcaute, C.R., Pérez-Iglesias, J.M., Nikoloff, N., et al., 2014. Genotoxicity evaluation of the insecticide imidacloprid on circulating blood cells of Montevideo tree frog *Hypsiboas pulchellus* tadpoles (Anura, Hylidae) by comet and micronucleus bioassays. *Ecol. Indic.* [J.] 45, 632–639.
- Decuzzi, P., Godin, B., Tanaka, T., et al., 2010. Size and shape effects in the biodistribution of intravascularly injected particles. *J. Control Release* [J.] 141, 320–327.
- Della Torre, C., Bergami, E., Salvati, A., et al., 2014. Accumulation and Embryotoxicity of Polystyrene Nanoparticles at Early Stage of Development of Sea Urchin Embryos *Paracentrotus lividus*. *Environ. Sci. Technol.* [J.] 48, 12302–12311.
- Doktorovova, S., Souto, E.B., Silva, A.M., 2014. Nanotoxicology applied to solid lipid nanoparticles and nanostructured lipid carriers - a systematic review of in vitro data. *Eur. J. Pharm. Biopharm.* [J.] 87, 1–18.
- Du, J., Hu, Y.Q., Li, Z., et al., 2024. Toxicity of polystyrene nanoplastics in the liver and intestine of normal and high-fat-diet juvenile zebrafish. *Environ. Toxicol. Chem.* [J.] 43, 147–158.
- Xiong, X., Zhang, K., Chen, X., Huahong, S., Luo, Z., Wu, C., 2018. Sources and distribution of microplastics in China's largest inland lake – Qinghai Lake. *Environ. Pollut.* [J.] 235, 899–906.
- Egessa, R., Nankabirwa, A., Basooma, R., et al., 2020. Occurrence, distribution and size relationships of plastic debris along shores and sediment of northern Lake Victoria. *Environ. Pollut.* [J.] 257, 113442.
- Estrela, F.N., Guimaraes, A.T.B., Silva, F.G., et al., 2021. Effects of polystyrene nanoplastics on *Ctenopharyngodon idella* (grass carp) after individual and combined exposure with zinc oxide nanoparticles. *J. Hazard. Mater.* [J.] 403.
- Farrell, P., Nelson, K., 2013. Trophic level transfer of microplastic: *mytilus edulis* (L.) to *Carcinus maenas* (L.). *Environ. Pollut.* [J.] 177, 1–3.
- Fishelson, L., 2006. Cytomorphological alterations of the thymus, spleen, head-kidney, and liver in cardinal fish (Apogonidae, Teleostei) as bioindicators of stress. *J. Morphol.* [J.] 267, 57–69.
- Forte, M., Iachetta, G., Tussellino, M., et al., 2016. Polystyrene nanoparticles internalization in human gastric adenocarcinoma cells. *Toxicol. Vitr.* [J.] 31, 126–136.
- Gray, A.D., Wertz, H., Leads, R.R., et al., 2018. Microplastic in two South Carolina Estuaries: Occurrence, distribution, and composition. *Mar. Pollut. Bull.* [J.] 128, 223–233.
- Habumugisha, T., Zhang, Z.X., Fang, C., et al., 2023. Uptake, bioaccumulation, biodistribution and depuration of polystyrene nanoplastics in zebrafish (*Danio rerio*). *Sci. Total Environ.* [J.] 893.
- Harding, S., 2016. Marine Debris: understanding, Preventing and Mitigating the Significant Adverse Impacts on Marine and Coastal Biodiversity[C]//. Secr. Conv. Biol. Divers.
- Hayes, T.B., Falso, P., Gallipeau, S., et al., 2010. The cause of global amphibian declines: a developmental endocrinologist's perspective. *J. Exp. Biol.* [J.] 213, 921–933.
- Hu, L.L., Su, L., Xue, Y.G., et al., 2016. Uptake, accumulation and elimination of polystyrene microspheres in tadpoles of *Xenopus tropicalis*. *Chemosphere* [J.] 164, 611–617.
- Jia, T.T., Nie, P.H., Xu, H.Y., 2024. Combined exposure of nano-titanium dioxide and polystyrene nanoplastics exacerbate oxidative stress-induced liver injury in mice by regulating the Keap1/Nrf2/ARE pathway. *Environ. Toxicol.* [J.] 1.
- Jin, Y., Xia, J., Pan, Z., et al., 2018. Polystyrene nanoplastics induce microbiota dysbiosis and inflammation in the gut of adult zebrafish. *Environ. Pollut.* [J.] 235, 322–329.
- Kai, Z., Xiong, X., Hongjuan, H., et al., 2017. Occurrence and characteristics of nanoplastic pollution in Xiangxi Bay of three gorges reservoir. *China Environ. Sci. Technol.* [J.] 51, 3794–3801.
- Kang, Z., Lin, J., Yang, T., et al., 2023. Accumulation characteristics and toxic effects of different functionalized nanoplastics in *Paphia undulata*. *Mar. Environ. Sci.* [J.] 42, 362–368.
- Khalid, N., Aqeel, M., Noman, A., et al., 2021. Interactions and effects of nanoplastics with heavy metals in aquatic and terrestrial environments. *Environ. Pollut.* [J.] 290, 118104.
- Khayoon, H.A., Ismael, Al-Nayili A, M., et al., 2023. Fabrication of LaFeO₃-nitrogen deficient g-C₃N₄ composite for enhanced the photocatalytic degradation of RhB under sunlight irradiation. *Inorg. Chem. Commun.* [J.] 157.
- Kim, J.H., Yu, Y.B., Choi, J.H., 2021. Toxic effects on bioaccumulation, hematological parameters, oxidative stress, immune responses and neurotoxicity in fish exposed to nanoplastics: A review. *J. Hazard Mater.* [J.] 413, 125423.
- Kullak-Ublick, G.A., Meier, P.J., 2000. Mechanisms of cholestasis. *Clin. Liver Dis.* [J.] 4, 357–385.
- Lacave, J.M., Vicario-Parés, U., Bilbao, E., et al., 2018. Waterborne exposure of adult zebrafish to silver nanoparticle and to ionic silver results in differential silver accumulation and effects at cellular and molecular levels. *Sci. Total Environ.* [J.] 642, 1209–1220.
- Lazaridis, K.N., Larusso, N.F., 2015. The Cholangiopathies. *Mayo Clin. Proc.* [J.] 90, 791–800.
- Lee, J.J., White, A.G., Rice, D.R., et al., 2013. In vivo imaging using polymeric nanoparticles stained with near-infrared chemiluminescent and fluorescent squaraine catenane endoperoxide. *Chem. Commun.* [J.] 49, 3016–3018.
- Li, Z.L., Feng, C.H., Wu, Y.H., et al., 2020. Impacts of nanoplastics on bivalve: fluorescence tracing of organ accumulation, oxidative stress and damage. *J. Hazard. Mater.* [J.] 392.
- Li, L., XU, M.J., He, C., et al., 2022. Polystyrene nanoplastics potentiate the development of hepatic fibrosis in high fat diet fed mice. *Environ. Toxicol.* [J.] 37, 362–372.
- Lu, Y., Zhang, Y., Deng, Y., et al., 2016a. Uptake and Accumulation of Polystyrene Microparticles in Zebrafish (*Danio rerio*) and Toxic Effects in Liver. *Environ. Sci. Technol.* [J.] 50, 4054–4060.
- Lu, Y., Zhang, Y., Deng, Y., et al., 2016b. Uptake and Accumulation of Polystyrene Microparticles in Zebrafish (*Danio rerio*) and Toxic Effects in Liver. *Environ. Sci. Technol.* [J.] 50, 4054–4060.
- Lusher A., Hollman P., Mendoza-Hill J.. Microplastics in fisheries and aquaculture: status of knowledge on their occurrence and implications for aquatic organisms and food safety[C]//FAO,2017.
- Migwi, F.K., Ogunah, J.A., Kiratu, J.M., 2020. Occurrence and Spatial Distribution of Microparticles in the Surface Waters of Lake Naivasha, Kenya. *Environ. Toxicol. Chem.* [J.] 39, 765–774.

- Mouchet, F., Gauthier, L., 2013. Genotoxicity of contaminants: amphibian micronucleus assays. *Encycl. Aquat. Toxicol. Compr. Handb. (Or. Pract. Guide) Ecotoxicological Terms* [J.] 2, 1221.
- Murphy, F., Quinn, B., 2018. The effects of microplastic on freshwater Hydra attenuata feeding, morphology & reproduction. *Environ. Pollut.* [J.] 234, 487–494.
- Najahi-Missaoui, W., Arnold, R.D., Cummings, B.S., 2020. Safe nanoparticles: are we there yet? *Int. J. Mol. Sci.* [J.] 22.
- North, E.J., Halden, R.U., 2013. Plastics and environmental health: the road ahead. *Rev. Environ. Health* [J.] 28, 1–8.
- Ozturk, I.C., Ozturk, F., Gul, M., et al., 2009. Protective effects of ascorbic acid on hepatotoxicity and oxidative stress caused by carbon tetrachloride in the liver of Wistar rats. *Cell Biochem Funct.* [J.] 27, 309–315.
- Pacheco, A., Martins, A., Guilhermino, L., 2018. Toxicological interactions induced by chronic exposure to gold nanoparticles and microplastics mixtures in *Daphnia magna*. *Sci. Total Environ.* [J.] 628–629, 474–483.
- Pandey, S., Parvez, S., Sayeed, I., et al., 2003. Biomarkers of oxidative stress: a comparative study of river Yamuna fish Wallago attu (Bl. & Schn). *Sci. Total Environ.* [J.] 309, 105–115.
- Peng, G., Zhu, B., Yang, D., et al., 2017. Microplastics in sediments of the Changjiang Estuary, China. *Environ. Pollut.* [J.] 225, 283–290.
- Prata, J.C., Costa, D.A., Lopes, J.P., 2020. Environmental exposure to microplastics: An overview on possible human health effects. *Sci. Total Environ.* [J.] 702, 134455.
- Rosenkranz, P., Chaudhry, Q., Stone, V., et al., 2009. A comparison of nanoparticle and fine particle uptake by *Daphnia magna*. *Environ. Toxicol. Chem.* [J.] 28, 2142–2149.
- Sharma, V., Anderson, D., Dhawan, A., 2012. Zinc oxide nanoparticles induce oxidative DNA damage and ROS-triggered mitochondria mediated apoptosis in human liver cells (HepG2). *Apoptosis* [J.] 17, 852–870.
- Shiye Z., Tao W., Lixin Z., et al. 2021. Corrigendum to ‘Analysis of suspended microplastics in the Changjiang Estuary: Implications for riverine plastic load to the ocean’ [Water Res. 161 (2019) 560–569/48672]. *Water Research* [J], 195: 116987–116987.
- Sussarellu, R., Suquet, M., Thomas, Y., et al., 2016. Oyster reproduction is affected by exposure to polystyrene microplastics. *Proc. Natl. Acad. Sci. USA* [J.] 113, 2430–2435.
- Verla, A.W., Enyoh, C.E., Verla, E.N., et al., 2019. Microplastic-toxic chemical interaction: a review study on quantified levels, mechanism and implication. *SN Appl. Sci.* [J.] 1, 1400.
- Wang, J., Li, Y., LU, L., et al., 2019. Polystyrene microplastics cause tissue damages, sex-specific reproductive disruption and transgenerational effects in marine medaka (*Oryzias melastigma*). *Environ. Pollut.* [J.] 254, 113024.
- Watts, A.J.R., Lewis, C., Goodhead, R.M., et al., 2014. Uptake and Retention of Microplastics by the Shore Crab *Carcinus maenas*. *Environ. Sci. Technol.* [J.] 48, 8823–8830.
- Wen, B., Jin, S.-R., Chen, Z.-Z., et al., 2018. Single and combined effects of microplastics and cadmium on the cadmium accumulation, antioxidant defence and innate immunity of the discus fish (*Symphysodon aequifasciatus*). *Environ. Pollut.* [J.] 243, 462–471.
- Xia, X., Sun, M., Zhou, M., et al., 2020. Polyvinyl chloride microplastics induce growth inhibition and oxidative stress in *Cyprinus carpio* var. larvae. *Sci. Total Environ.* [J.] 716, 136479.
- Xing, H., Wang, Z., Gao, X., et al., 2015. Atrazine and chlorpyrifos exposure induces liver autophagic response in common carp. *Ecotoxicol. Environ. Saf.* [J.] 113, 52–58.
- Xiong, Wu, X., Elser J J, C., et al., 2019. Occurrence and fate of microplastic debris in middle and lower reaches of the Yangtze River – From inland to the sea. *Sci. Total Environ.* [J.] 659, 66–73.
- Yang, H., Xiong, H., MI, K., et al., 2020. Toxicity comparison of nano-sized and micron-sized microplastics to Goldfish *Carassius auratus* Larvae. *J. Hazard. Mater.* [J.] 388, 122058.
- Yasin, N.A.E., El-Naggar, M.E., Ahmed, Z.S.O., et al., 2022. Exposure to Polystyrene nanoparticles induces liver damage in rat via induction of oxidative stress and hepatocyte apoptosis. *Environ. Toxicol. Pharmacol.* [J.] 94, 103911.
- Yu, P., Liu, Z., Wu, D., et al., 2018. Accumulation of polystyrene microplastics in juvenile *Eriocheir sinensis* and oxidative stress effects in the liver. *Aquat. Toxicol.* [J.] 200, 28–36.
- Zaman, M., Khan, F.U., Younas, W., et al., 2024. Physiological and histopathological effects of polystyrene nanoparticles on the filter-feeding fish *Hypophthalmichthys molitrix*. *Sci. Total Environ.* [J.] 912, 169376.
- Zhang, Q., Qu, Q., LU, T., et al., 2018. The combined toxicity effect of nanoplastics and glyphosate on *Microcystis aeruginosa* growth. *Environ. Pollut.* [J.] 243, 1106–1112.
- Zielińska, A., Costa, B., Ferreira, M.V., et al., 2020. Nanotoxicology and nanosafety: safety-by-design and testing at a glance. *Int. J. Environ. Res Public Health* [J.] 17.
- Zinatloo-Ajabshir, S., Rakshan, S., Mehrabadi, Z., et al., 2024b. Novel rod-like [Cu (phen)(2)(OAc)]-PF(6) complex for high-performance visible-light-driven photocatalytic degradation of hazardous organic dyes: DFT approach, Hirshfeld and fingerprint plot analysis. *J. Environ. Manag.* [J.] 350, 119545.
- Zinatloo-Ajabshir, S., Rakshan, S., Mehrabadi, Z., et al., 2024a. Novel rod-like [Cu (phen)(2)(OAc)]-PF(6) complex for high-performance visible-light-driven photocatalytic degradation of hazardous organic dyes: DFT approach, Hirshfeld and fingerprint plot analysis. *J. Environ. Manag.* [J.] 350, 119545.
- Zinatloo-Ajabshir, S., Salavati-Niasari, M., 2019. Preparation of magnetically retrievable CoFe2O4@ SiO2@ Dy2Ce2O7 nanocomposites as novel photocatalyst for highly efficient degradation of organic contaminants. *Compos. Part B: Eng.* [J.] 174, 106930.
- Zinatloo-Ajabshir, Z., Zinatloo-Ajabshir, S., 2019. Preparation and characterization of curcumin niosomal nanoparticles via a simple and eco-friendly route. *J. Nanostruct.* [J.] 9, 784–790.